Laser and Particle Beams (2012), *30*, 319–324.
© Cambridge University Press, 2012 0263-0346/12 $20.00
doi:10.1017/S0263034612000171

Charge effect in secondary electron emission from silicon surface induced by slow neon ions

ZHONGFENG XU,[1,2,3] LIXIA ZENG,[1,2,4] YONGTAO ZHAO,[1,3] JIANGUO WANG,[1,2] YUYU WANG,[3] XIAOAN ZHANG,[3,4] GUOQING XIAO,[1,3] AND FULI LI[1,2]

[1]HCI Joint Center of Xi'an Jiaotong University and Institute of Modern Physics, China
[2]Department of Applied Physics, Xi'an Jiaotong University, Xi'an, China
[3]Institute of Modern Physics, Chinese Academy of Science, Lanzhou, China
[4]School of Physics and Electronic Engineering, Xianyang Normal University, Xianyang, China

(Received 26 October 2011; Accepted 28 October 2011)

Abstract

Total electron emission yield for impact of slow $Ne^{q+}(q = 2, 4, 6, 8)$ ions with various kinetic energy under normal incidence on *n*-type Si has been measured. It is shown that for the same charge state, the total electron yield γ increases linearly as the kinetic energy of projectile at impact increases, up to velocities corresponding to the "classical" threshold. Separation of kinetic electron yield γ_{KE} and potential electron yield γ_{PE} shows that γ_{PE} is proportional to the ion charge state and γ_{KE} increases linearly with projectile velocity. Finally, based on "single hole without hopping" hypothesis, the expression of the "CRF" *F(q)* is given, and the relation between γ_{KE} and q is obtained successfully for the first time, which is also a basis for judging whether the "trampoline effect" exists.

Keywords: Charge restrain factor; Electron emission yield; Highly charged ions (HCI); Threshold velocity

1. INTRODUCTION

The interaction of intense radiation and charged particles with solid surfaces is an intensively investigated field (Pikuz *et al.*, 2010; Kumar & Verma, 2011; Zhu *et al.*, 2011). The underlying physical processes are of great interest not only for basic research, but also for technological applications such as material modifications, X-rays source devices, radiation physics, chemistry, biology, plasma-wall interactions, and surface analysis as well (Lucio *et al.*, 2006; Bajales *et al.*, 2008; Hoffmann *et al.*, 2005, 2007; Kudo *et al.*, 2000; Rosmej *et al.*, 2005). We will here concentrate on the effect of secondary electron emission (SEE) from surfaces under ion bombardment. This effect has been extensively studied during several decades because of its fundamental and technological importance. Secondary electron emission from surface is commonly ascribed to two different mechanisms, the potential emission process (PE) (Hagstrum, 1954) and the kinetic emission process (KE) (Baragiola, 1994). However, separation of the relative contribution of potential and kinetic processes to the total electron emission is not an easy task. Several attempts have been made previously (Lemell *et al.*, 1998). Hughes *et al.* (1993) attempted to separate PE and KE via coincidence measurements of electron emission and the angular distribution of scattered projectiles, Stöckl *et al.* (2004), or to subtract the KE contribution from measurements of grazing scattering (incident angle $< 4^{\circ}$) of Ar ions from LiF (001) surface. Lederer *et al.* (2003) studied the threshold behavior of KE by measuring the yield for neutral projectile impact on Al surface.

In this paper, we present experimental results for electron emission yield of $Ne^{q+}(q = 2, 4, 6, 8)$ impacting on Si at normal incidence. The mechanism of electron emission is investigated as a function of charge state and we discuss how charge states impact the relative importance of potential electron emission (PEE) versus kinetic electron emission (KEE).

2. EXPERIMENTAL SETUP

The highly charged ions used for this experiment were produced by 14.5GHz electron cyclotron resonance ion source (ECRIS) at the Heavy Ion Research Facility in Lanzhou (HIRFL) (Zhao *et al.*, 2009). Figure 1 shows the recently constructed experimental setup for secondary electron yield measurements.

Address correspondence and reprint requests to: Zhongfeng Xu, Department of Applied Physics, Xi'an Jiaotong University, Xi'an, China. E-mail: zhfxu@mail.xjtu.edu.cn

https://doi.org/10.1017/S0263034612000171 Published online by Cambridge University Press

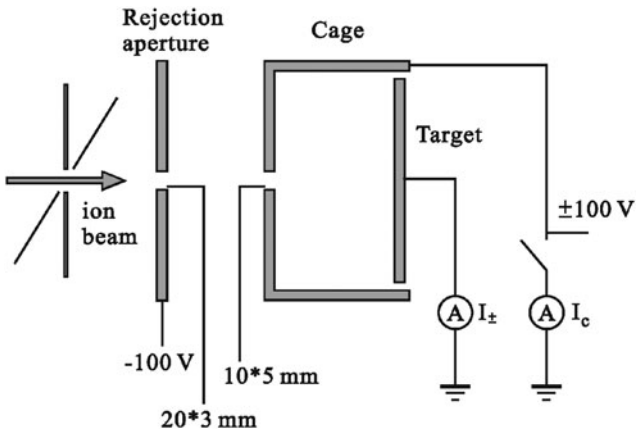


Fig. 1. Schematic diagram of the experimental setup used for measuring the total electron yield.

It consists of three major parts namely, an adjustable beam collimator, a rejection aperture (20 mm × 3 mm) and a cage. The beam defining collimator serves to prevent the incoming ions from directly impacting the rejection aperture and has a diameter of 2 mm. The cage that is operated with a voltage of ±100 V surrounds the target in order to collect or to suppress electrons emitted from the target. The cage has an aperture of 10 mm × 5 mm for ion beam entrance, through which the incident ion beam is collimated down to 2 mm in diameter, before it is able to reach the target surface. A rejection electrode at a potential of −100V is placed before the cage that prevents electrons from escaping and thus further enhances the electron collection efficiency. The current at the target is measured with a pico-ampere meter. When applying +100V to the cage with respect to the target, the total current

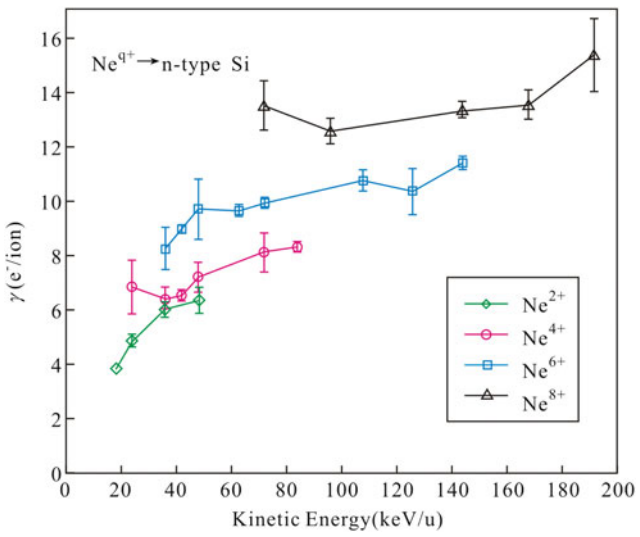


Fig. 2. (Color online) Total electron yield as a function of projectile kinetic energy for Ne^{q+}(q = 2, 4, 6, 8) impact on n-type Si in the normal incident case.

I_+ that is measured at the target consists of two components, the current of incoming ions I_i and the current of emitted electrons I_e.

$$I_+ = I_i + I_e = I_i + \gamma(I_i/q). \tag{1}$$

For −100V applied to the cage leads to a target current I_- that is equal to the incoming ion current.

$$I_- = I_i. \tag{2}$$

Therefore, the total electron yield is given as

$$\gamma = \frac{I_e}{I_i/q} = q\frac{I_+ - I_-}{I_-}. \tag{3}$$

Highly charged ion beam, with ion current in the range of 50–400 nA, were focused and collimated to a diameter of 3 mm. The target was mechanically polished and placed perpendicular to the ion-beam direction. The pressure in the target chamber was maintained at about 10^{-10} mbar. In order to obtain the required clean surface, a self-sputtering process was performed using Ar^+ ions. During the cleaning process, the surface condition was checked by measuring the electron yield at intervals and the experiment was started after achieving a stable electron yield.

3. RESULTS AND DISCUSSION

Figure 2 represents total electron yield as a function of projectile kinetic energy for Ne^{q+}(q = 2, 4, 6, 8) impact on n-type Si in the normal incident case results show that the total electron yield increases as the projectile kinetic energy and charge state q increase.

Total yield γ is divided into two parts, one is kinetic electron yield γ_{KE} , and the other is potential electron yield γ_{PE}. γ_{KE} almost vanishes at velocities v below "classical" KE threshold velocity v_{th} (Baragiola *et al.*, 1979). When $v > v_{th}$, there is an approximate linear relationship between γ_{KE} and v_{th} (Hughes *et al.*, 1993; Vana *et al.*, 1995):

$$\gamma_{KE} = k(v - v_{th})\Theta(v - v_{th}), \tag{4}$$

where Θ $(v - v_{th})$is a step function starting at the KE threshold velocity v_{th}. According to Baragiola *et al.* (1979),

$$v_{th} = \frac{v_F}{2}[(1 + W_\phi/E_F)^{1/2} - 1], \tag{5}$$

where $W_\varphi = 4.85$ eV, $E_F = 12.43$ eV for the target n-type Si (Michaelson, 1977), then we get that $v_{th} = 1.87 \times 10^5$ m/s. In Figure 3, total electron yield as a function of v is shown with a linear least-squares fit to the data. The fit variance is 0.6%, 7.3%, 4.8%, and 8.2% for q = 2,4,6,8, respectively.

If subtracting the potential yield γ_{PE} from the total electron yield γ, we will get the kinetic electron yield which will be

https://doi.org/10.1017/S0263034612000171 Published online by Cambridge University Press

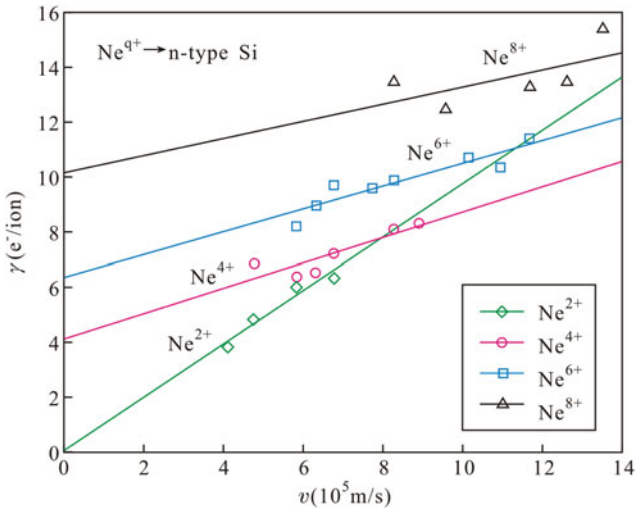


Fig. 3. (Color online) Total electron yield as a function of projectile velocity, the solid lines are linear least-squares fits to the experiment data points.

equal to zero when $v = v_{th}$ (Baragiola, 1994). Therefore when $v = v_{th}$, the potential electron yield γ_{PE}, listed in Table 1, is equal to the total electron yield γ.

Potential electron yield consists of two parts, one is inversely proportional to $\sqrt{v}$ and the other is a velocity-independent value γ_∞ (Kurz *et al.*, 1993, 1992).

$$\gamma_{PE} = c_1/\sqrt{v} + \gamma_\infty, \tag{6}$$

where c_1 is a constant. Kinetic electron emission does not yield more than 0.5 electron/ion at projectile velocity v below 2×10^5m/s (Lakits *et al.*, 1990; Winter *et al.*, 1991). Electron emission measurement for impact of projectile with v between 1×10^4 m/s and 1.5×10^5 m/s by Kurz

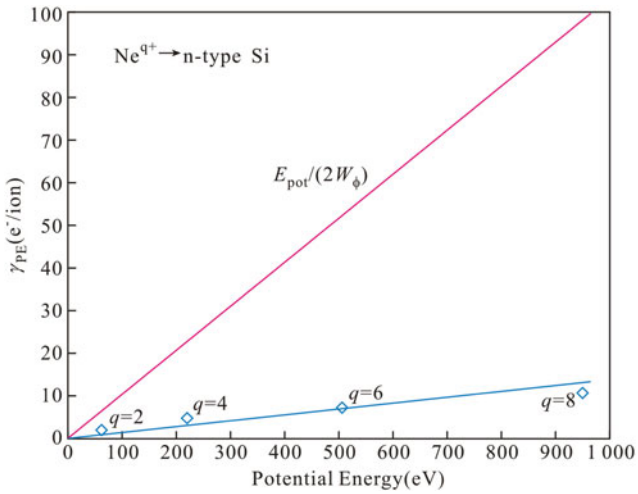


Fig. 4. (Color online) Pure potential electron emission contribution as a function of available potential energy compared to model predictions under normal impact

Table 1. *Potential electron yield,* k *and* E_{pot} *for various q*

q	$\gamma_{PE}(q)$ / e$^-$/ion	K	E_{pot} / eV
2	1.83	0.97	59
4	4.95	0.46	218
6	7.09	0.42	502
8	10.74	0.31	945

et al. (1993, 1992) proposes that yield (almost potential electron) first decrease gradually and then level off towards γ_∞. We therefore assume that the first term of Eq. (6) is negligible small for evolution of γ_{PE} when v even higher than v_{th} thus yield

$$\gamma_{PE} \approx \gamma_\infty. \tag{7}$$

Through linear fitting the data of γ_{PE} and q in Table 1, the relation between γ_{PE} and q can be shown by Eq. (8), the fit variance is 0.2%.

$$\gamma_{PE} \approx \gamma_\infty = 1.44q - 1.06. \tag{8}$$

That means the potential electron yield γ_{PE} is proportional to ion charged state and γ_{PE} is independent of the projectile velocity. The linear increase of the contributions γ_∞ with q is agreement with the arguments put forward by Stöckl *et al.* (2004) and Kurz *et al.* (1992) for Ar^{q+}-Xe^{q+}-Hg^{q+} impacting on Au-LiF-CaF_2. All these processes require a minimum potential energy of at least twice the binding energy W_ϕ of the highest occupied state of the solid. The maximum possible number of electrons n_{max} emitted via PE is therefore given by (Stöckl *et al.*, 2004)

$$n_{max} = E_{pot}/2W_\phi, \tag{9}$$

where the E_{pot} is the potential energy of projectile, which is listed in Table 1 for $q = 2$, 4, 6, 8, respectively.

In Figure 4, the potential electron yield γ_{PE} is compared to maximum possible number of electrons n_{max}, result shows that γ_{PE} is much smaller than n_{max}, i.e., not all of the potential energy is used for electron emission. The result is sharp contrast to the result of grazing impact of multiply charged Ar Ions on a LiF(001) surface (Stöckl *et al.*, 2004) which shows that a practically all of the available potential energy is used for electron emission during grazing scattering. However, in case of normal impact, our result is consistent with Vana *et al.* (1995). Part of the potential energy can be used to emit electron because of non-complete deexcitation and incomplete neutralization. It is found in our experiment that, the fraction of potential energy which is used for electron emission is about 30%, 21%, 14%, 11% for $q = 2$, 4, 6, 8, respectively, and the projectile velocity almost does not affect the potential electron yield.

https://doi.org/10.1017/S0263034612000171 Published online by Cambridge University Press

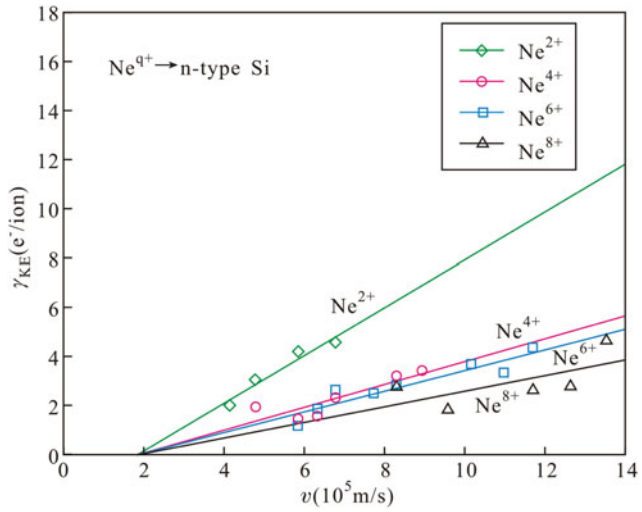


Fig. 5. (Color online) The kinetic electron yield γ_{KE} for impact of Ne^{q+}(q = 2, 4, 6, 8) on Si surface, through deducing γ_{PE} in Figure 3.

In Figure 3, shifting down the yield-velocity curves for each q and making them intersect exactly at threshold velocity v_{th}, we get the kinetic electron yield γ_{KE} curves as a function of velocity in Fig.5.

In Figure 5, the results show that γ_{KE} increases linearly with projectile velocity and γ_{KE} is smaller for higher charge state at the same impact velocity. Meanwhile, both Figure 5 and Table 1 show that the value of k in Eq. (4) is tends to be smaller when q increases, i.e., charge state can restrain kinetic electron emission (KEE). Similar results were obtained in the experiment of impacting Ne^{q+} on Au surface by Vana *et al.* (1995). Our results are not contradictory with the conclusion (Baragiola *et al.*, 1979; Schou, 1980) that the higher the observed energy loss, the higher will be the kinetic electron yield, due to electron vacancies occurring on the solid surface for neutralization during the approach of the ion to the surface. Higher charge state of projectile can induce more such vacancies, thus there may be many holes at the same site. On the one hand, the holes can reduce the collision velocity of projectile and decrease the energy loss of projectile interacting with surface consequently. On the other hand, because of potential barrier of holes acting on electron, the escape capability of kinetic emission electron decreases. Due to these two reasons, the kinetic electron emission decreases with the increasing of charge state, which can be used to explain "trampoline effect" (Wirtz *et al.*, 2003; Briand *et al.*, 1996). For slow projectiles and normal incidence, the ionic motion depends sensitively on the interplay between image acceleration toward the surface and repulsion by an ensemble of positive holes charges in the surface. The repulsive interaction between the holes and the projectile can become stronger than the attractive self-image force and eventually lead to the backscattering of a still multiply charged ion high above the surface without touching it.

So we can express kinetic electron yield as the sum of two parts, one is relevant with charge state and the other is independent of the charge state.

$$\gamma_{KE} = \gamma^0_{KE} - \gamma^0_{KE}F(q). \tag{10}$$

Where the γ^0_{KE} is the kinetic electron yield for neutral projectile, $F(q)$ is a function of q to be named Charge Restrain Factor (CRF), obviously $F(0) = 0$. Figure 5 shows that the kinetic electron yield is proportional to projectile velocity, so the relation between change state q and projectile velocity v can be used to reflect the relation between change state q and kinetic electron yield γ_{KE}. If we assume that there are relatively stable holes on the surface, the repulsive force the holes act on the projectile and projectile velocity are along the normal direction of the surface and there are only single holes interact with projectile, the repulsive force can be given by

$$f_{corr} = \frac{Q_{eff}e^2}{\varepsilon_0 R_z^2}, \tag{11}$$

where ε_0 is the permittivity of vacuum, R_z is the distance between projectile and solid surface, and Q_{eff} is the effective charge of projectile while interacting with holes, which is an R_z-related parameter and decreases with decreasing R_z. The potential electron emission induced by incoming ions, that is the incoming ions capture electrons and lose their positive charges, occurs when R_z reaches a critical distance z_c, depending on the charge state q of incident ions and the work function of target ϕ.

$$z_c(\text{Å}) = 20.3\phi^{-1}(q + 0.25)^{1/2}. \tag{12}$$

Assuming the charges carried with incident ions are released completely when R_z reaches z_f and proportional to R_z ranging from z_c to z_f. Thus Q_{eff} can be given by

$$Q_{eff} = \begin{cases} q(R_z - z_f)/(z_c - z_f) & , z_f \le R_z \le z_c \\ q & , R_z > z_c \end{cases} \tag{13}$$

We only consider kinetic energy change caused by f_{corr}, because the kinetic energy loss in other ways is not caused by holes directly, then

$$\frac{M_p}{2}\left(v_p^2 - v_p'^2\right) = \int_{z_i}^{z_c} \frac{qe^2(R_2 - z_f)}{\varepsilon_0(z_c - z_f)R_z^2}dR_z + \int_{z_c}^{\infty} \frac{qe^2}{\varepsilon_0 R_z^2}dR_z, \tag{14}$$

$$\frac{m_u}{2}\left(v_P^2 - v_P'^2\right) = \frac{qe^2}{\varepsilon_0 Z_P}\left(\frac{1}{z_c} + \frac{\ln(z_c/z_f) + z_f/z_c - 1}{z_c - z_f}\right), \tag{15}$$

where M_P is projectile mass, m_u is nucleon mass, Z_P is atomic number of projectile. The reduction of kinetic electron yield

https://doi.org/10.1017/S0263034612000171 Published online by Cambridge University Press

caused by charge state can be given by

$$\Delta\gamma_{KE} = \gamma^0_{KE}F(q) = \beta_q \frac{qe^2}{\varepsilon_0 Z_P}\left(\frac{1}{z_c} + \frac{\ln(z_c/z_f) + z_f/z_c - 1}{z_c - z_f}\right). \quad (16)$$

Then

$$F(q) = \beta_q \frac{qe^2}{\varepsilon_0 Z_P}\left(\frac{1}{z_c} + \frac{\ln(z_c/z_f) + z_f/z_c - 1}{z_c - z_f}\right)\Big/\gamma^0_{KE}, \quad (17)$$

where β_q is a parameter and is independent of the charge state q. From Eq. (17), we can easily conclude that $F(q)$ as a function of q increases with the charge state q. Meanwhile, at the same state, the larger of the atomic number of projectile Z_P, the harder for the charge state to improve the projectile velocity, so $F(q)$ is inversely proportional to Z_P. Finally, the smaller of z_c, the longer of projectile stays in high charge state, so the larger repulsive force the holes act on projectile, this is consist with that $F(q)$ becomes larger with the decrease of z_c. In conclusion, the expression of $F(q)$ in Eq. (17) is reasonable. Then the γ_{KE} is given by

$$\gamma_{KE} = \gamma^0_{KE} - \frac{\beta_q qe^2}{\varepsilon_0 Z_P}\left(\frac{1}{z_c} + \frac{\ln(z_c/z_f) + z_f/z_c - 1}{z_c - z_f}\right). \quad (18)$$

The relation between γ_{KE} and q is given successfully. From Eq. (18), it can be easily found that if the second term in the right side is big enough, γ_{KE} will be smaller than zero. This case is called "trampoline effect", and the critical condition for trampoline effect is $\gamma_{KE} = 0$.

4. CONCLUSION

Experimental results of impacting $Ne^{q+}(q = 2, 4, 6, 8)$ on Si at normal incidence are reported and electron emission yield has been discussed systematically. The results show that the potential electron yield γ_{PE} is proportional to ion charge state and γ_{PE} is independent of the projectile velocity, where the fit variance is 0.2%. The kinetic electron yieldγ_{KE} increases linearly with projectile velocity. Meanwhile, we find charge state can restrain kinetic electron emission. Finally, we give the expression of the "CRF" $F(q)$ based on "single-hole without hopping" hypothesis. And the relation between γ_{KE} and q is given successfully, which is also a basis for judging whether "trampoline effect" exists.

ACKNOWLEDGMENTS

Helpful contributions from Professor Dieter H.H Hoffmann are sincerely acknowledged. We also acknowledge technical support from the group of the 320 kV HCI platform at IMP-Lanzhou. This work was supported by the NSFC project in China (Grant Nos.11075125, 11075135, 11075192) and partially supported by the WTZ project (Grant No. 1390).

REFERENCES

Bajales, N., Cristina, L., Mendoza, S., Baragola, R.A., Goldberg, E.C. & Ferrón, J. (2008). Exciton autoionization in ion induced electron emission. *Phys. Rev. Lett.* **100**, 227604-1-4.

Baragiola, R.A. (1994). *Low Energy Ion Surface Interaction*. New York: Wiley.

Baragiola, R.A., Alonso, E.V. & Oliva Florio, A. (1979). Electron emission from clean metal surfaces induced by low-energy light ions. *Phys. Rev. B* **19**, 121–129.

Briand, J.P., Thuriez, S., Giardino, G., Borsoni, G., Froment, M., Eddrief, M. & Sebenne, C. (1996). Observation of hollow atoms or ions above insulator and metal surfaces. *Phys. Rev. Lett.* **77**, 1452–1455.

Hagstrum, H.D. (1954). Theory of auger ejection of electron from metals by ions. *Phys. Rev.* **96**, 336–365.

Hoffmann, D.H.H., Blazevic, A., Ni, P., Rosmej, O., Roth, M., Tahir, N., Tauschwitz, A., Udrea, S., Varentsov, D., Weyrich, K. & Maron, Y. (2005). Present and future perspectives for high energy density physics with intense heavy ion and laser beams. *Laser Part. Beams* **23**, 47–53.

Hoffmann, D.H.H., Blazevic, A., Korostiy, S., Ni, P., Pikuz, S.A., Rosmej, O., Roth, M., Tahir, N.A., Udrea, S., Varentsov, D., Weyrich, K., Sharkov, B.Y. & Maron, Y. (2007). Inertial fusion energy issues of intense heavy ion and laser beams interacting with ionized matter studied at GSI-Darmstadt. *Nucl. Instr.& Meth. Phys. Res. Sec. A* **577**, 8–13.

Hughes, I.G., Burgdörfer, J., Folkerts, L., Havener, C.C., Overbury, S.H., Robinson, M.T., Zehner, D.M., Zeijlmans Van Emmichoven, P.A. & Meyer, F.W. (1993). Separation of kinetic and potential electron emission arising from slow multicharged ion-surface interactions. *Phys. Rev. Lett.* **71**, 291–294.

Kudo, M., Sakai, Y. & Ichinokawa, T. (2000). Dependencies of secondary electron yields on work function for metals by electron and ion bombardment. *Appl. Phys. Lett.* **76**, 3475–3477.

Kumar, A. & Verma, A.L. (2011). Nonlinear absorption of intense short pulse laser over a metal surface embedded with nanoparticles. *Laser Part. Beams* **29**, 333–338.

Kurz, H., Aumayr, F., Lemell, C., Töglhofer, K. & Winter, HP. (1993). Neutralization of slow multicharged ions at a clean gold surface: total electron yields. *Phys. Rev. A* **48**, 2182–2191.

Kurz, H., Töglhofer, K., Winter, HP. & Aumayr, F. (1992). Electron emission from slow hollow atoms at a clean metal surface. *Phys. Rev. Lett.* **69**, 1140–1143.

Lakits, G., Aumayr, F., Heim, M. & Winter, HP. (1990). Threshold of ion-induced kinetic electron emission from a clean metal surface. *Phys. Rev. A* **42**, 5780–5783.

Lederer, S., Maass, K., Blauth, D., Winter, HP. & Aumayr, F. (2003). Kinetic electron emission from the selvage of a free-electron-gas metal. *Phys. Rev. B* **67**, 121405-1-4.

Lemell, C., Stöckl, J., Burgdörfer, J., Betz, G., Winter, HP. & Aumayr, F. (1998). Multicharged ion impact on clean Au(111): suppression of kinetic electron emission in glancing angle scattering. *Phys. Rev. Lett.* **81**, 1965–1968.

Lucio, O.G., Gavin, J. & Dubois, R.D. (2006). Differential electron emission for single and multiple ionization of argon by 500 eV positrons. *Phys. Rev. Lett.* **97**, 243201-1-4.

Michaelson, H.B. (1977). The work function of the elements and its periodicity. *J. Appl. Phys* **48**, 4729–4733.

Pikuz, S.A., Chefonov, O.V., Gasilov, S.V., Komarov, P.S., Ovchinnikov, A.V., Skobelev, I.YU., Ashitkov, S.YU.,

https://doi.org/10.1017/S0263034612000171 Published online by Cambridge University Press

Agranat, M.V., Zigler, A. & Faenov, A. YA. (2010). Micro-radiography with laser plasma X-ray source operating in air atmosphere. *Laser Part. Beams* **28**, 393–397.

Rosmej, O.N., Pikuz, S.A., Korostiy, S., Blazevic, A., Brambrink, E., Fertman, A., Mutin, T., Efremov, V.P., Pikuz, T.A., Faenov, A.Y., Loboda, P., Golubev, A.A. & Hoffmann, D.H.H. (2005). Radiation dynamics of fast heavy ions interacting with matter. *Laser Part. Beams* **23**, 79–85.

Schou, J. (1980). Transport theory for kinetic emission of secondary electrons from solids. *Phys. Rev. B* **22**, 2141–2174.

Stöckl, J., Suta, T., Ditroi, F., Winter, HP. & Aumayr, F. (2004). Separation of potential and kinetic electron emission for grazing impact of multiply charged Ar ions on a LiF(001) surface. *Phys. Rev. Lett.* **93**, 263201-1-4.

Vana, M., Kurz, H., Winter, HP. & Aumayr, F. (1995). Potential and kinetic electron emission from clean gold induced by multicharged nitrogen ions. *Nucl. Instr. and Meth. in Phys. Res. B* **100**, 402–406.

Winter, HP., Aumayr, F. & Lakits, G. (1991). Recent advances in understanding particle-induced electron emission from metal surfaces. *Methods Phys. Res., Sect. B* **58**, 301–308.

Wirtz, L., Reinhold, CO., Lemell, C. & Burgdörfer, J. (2003). Liouville master equation for multielectron dynamics: Neutralization of highly charged ions near a LiF surface. *Phys. Rev. A* **67**, 012903-1-19.

Zhao, Y.T., Xiao, G.Q., Xu, H.S., Zhao, H.W., Xia, J.W., Jin, G.M., Ma, X.W., Liu, Y., Yang, Z.H., Zhang, P.M., Wang, Y.Y., Li, D.H., Zhao, H.Y., Zhan, W.L., Xu, Z.F., Zhao, D., LI, F.L. & Chen, X.M. (2009). An outlook of heavy ion driven plasma research at IMP-Lanzhou. *Nucl. Instr. & Meth. Phys. Res. Sec. B* **267**, 163–166.

Zhu, X.P., Zhang, F.G., Tang, Y., & Lei, M.K. (2011). Phase transformation under beam-target interactions during high-intensity pulsed ion beam irradiation at low pressure. *Laser Part. Beams* **29**, 283–289.

https://doi.org/10.1017/S0263034612000171 Published online by Cambridge University Press